

# Platinum–osmium isotope evolution of the Earth’s mantle: Constraints from chondrites and Os-rich alloys

A.D. Brandon <sup>a,\*</sup>, R.J. Walker <sup>b</sup>, I.S. Puchtel <sup>b</sup>

<sup>a</sup> NASA Johnson Space Center, Mail Code KR, Building 31, Houston, TX 77058, USA

<sup>b</sup> Isotope Geochemistry Laboratory, Department of Geology, University of Maryland, College Park, MD 20742, USA

Received 6 September 2005; accepted in revised form 13 January 2006

## Abstract

Separation of a metal-rich core strongly depleted the silicate portion of the Earth in highly siderophile elements (HSE), including Pt, Re, and Os. To address the issues of how early differentiation, partial melting, and enrichment processes may have affected the relative abundances of the HSE in the upper mantle,  $^{187}\text{Os}/^{188}\text{Os}$  and  $^{186}\text{Os}/^{188}\text{Os}$  data for chondrites are compared with data for Os-rich alloys from upper mantle peridotites. Given that  $^{187}\text{Os}$  and  $^{186}\text{Os}$  are decay products of  $^{187}\text{Re}$  and  $^{190}\text{Pt}$ , respectively, these ratios can be used to constrain the long-term Re/Os and Pt/Os of mantle reservoirs in comparison to chondrites. Because of isotopic homogeneity, H-group ordinary and other equilibrated chondrites may be most suitable for defining the initial  $^{186}\text{Os}/^{188}\text{Os}$  of the solar system. The  $^{186}\text{Os}/^{188}\text{Os}$  ratios for five H-group ordinary chondrites range only from 0.1198384 to 0.1198408, with an average of  $0.1198398 \pm 0.0000016$  ( $2\sigma$ ). Using the measured Pt/Os and  $^{186}\text{Os}/^{188}\text{Os}$  for each chondrite, the calculated initial  $^{186}\text{Os}/^{188}\text{Os}$  at 4.567 Ga is  $0.1198269 \pm 0.0000014$  ( $2\sigma$ ). This is the current best estimate for the initial  $^{186}\text{Os}/^{188}\text{Os}$  of the bulk solar system. The mantle evolution of  $^{186}\text{Os}/^{188}\text{Os}$  can be defined via examination of mantle-derived materials with well-constrained ages and low Pt/Os. Two types of mantle-derived materials that can be used for this task are komatiites and Os-rich alloys. The alloys are particularly valuable in that they have little or no Re or Pt, thus, when formed, evolution of both  $^{187}\text{Os}/^{188}\text{Os}$  and  $^{186}\text{Os}/^{188}\text{Os}$  ceases. Previously published results for an Archean komatiite and new results for Os-rich alloys indicate that the terrestrial mantle evolved with Pt–Os isotopic systematics that were indistinguishable from the H-group ordinary and some enstatite chondrites. This corresponds to a Pt/Os of  $2.0 \pm 0.2$  for the primitive upper mantle evolution curve. This similarity is consistent with previous arguments, based on the  $^{187}\text{Os}/^{188}\text{Os}$  systematics and HSE abundances in the mantle, for a late veneer of materials with chondritic bulk compositions controlling the HSE budget of the upper mantle. It is very unlikely that high pressure metal–silicate segregation leading to core formation can account for the elemental and isotopic compositions of HSE in the upper mantle.

© 2006 Elsevier Inc. All rights reserved.

## 1. Introduction

The Re–Os and Pt–Os isotope systems can provide robust constraints on the mechanisms that controlled the abundances of highly siderophile elements (HSE: Re, Au, Os, Ir, Rh, Ru, Pt, and Pd) in the Earth’s mantle from its earliest differentiation history to the present. The isotope  $^{187}\text{Re}$  decays via beta emission to  $^{187}\text{Os}$  with  $\lambda = 1.67\text{E}^{-11} \text{ yr}^{-1}$ , and  $^{190}\text{Pt}$  decays via alpha emission to

$^{186}\text{Os}$  with  $\lambda = 1.48\text{E}^{-12} \text{ yr}^{-1}$  (Begemann et al., 2001; Smoliar et al., 1996). The present-day  $^{187}\text{Os}/^{188}\text{Os}$  in the primitive upper mantle (PUM) estimated from mantle peridotites is  $0.1296 \pm 0.0008$  (Meisel et al., 2001). This value is indistinguishable from the averages of  $^{187}\text{Os}/^{188}\text{Os}$  in enstatite and ordinary chondrites, and implies that the PUM evolved with a Re/Os ratio within the range of these chondrite groups. This is the best constrained time-integrated ratio for the relative elemental abundances of any HSE within the mantle.

The Pt–Os isotopic system can be used to place constraints on the long-term Pt/Os of the mantle in a manner similar to what has been achieved for Re/Os. This system

\* Corresponding author. Fax: +1 281 483 1573.

E-mail address: [alan.d.brandon1@jsc.nasa.gov](mailto:alan.d.brandon1@jsc.nasa.gov) (A.D. Brandon).

has an advantage over the Re/Os system in trying to establish a mantle ratio for two HSE in that under conditions of partial melting in the mantle, the liquid silicate/solid silicate partition coefficients for Re, Pt, and Os are  $\sim 0.1$ ,  $\sim 1$  and slightly greater than 1, respectively (Hauri and Hart, 1997; Walker et al., 1999; Rehkämper et al., 1999; Puchtel and Humayun, 2000). This means that during low degree partial melting in the mantle, Pt and Os fractionate much less from one another than Re and Os will. Only during large degrees of melting that produces komatiitic magma, is Pt significantly depleted in the solid residue relative to Os (Puchtel et al., 2004b). Thus, random samples of the mantle, or mantle-derived materials, may provide a more accurate and uniform insight into the  $^{186}\text{Os}/^{188}\text{Os}$  of the mantle than the same samples can do for  $^{187}\text{Os}/^{188}\text{Os}$ . This system does, however, come with a penalty. The atomic abundance of  $^{190}\text{Pt}$  is very low (0.0129%) and the half-life for it is quite large ( $\sim 450$  Ga). This results in very little growth in  $^{186}\text{Os}$  over solar system history in most materials, requiring very high measurement precision. Nonetheless, provided the  $^{186}\text{Os}/^{188}\text{Os}$  of mantle derived materials can be measured to sufficient precision, the system can be used to precisely constrain Pt/Os without extrapolations from variably melt depleted samples as is required for Re/Os.

Osmium-rich grains are found as inclusions in chromite or in placers downstream from ultramafic massifs (Cabri and Harris, 1975; Stockman and Hlava, 1984; Cabri et al., 1996). These grains are alloys typically composed of Os, Ir, and Ru, with insignificant amounts of other elements, and are ideal candidates for precise  $^{186}\text{Os}$  measurements (Hattori and Hart, 1991; Walker et al., 1997; Brandon et al., 1998; Bird et al., 1999; Meibom and Frei, 2002; Meibom et al., 2002; Malitch, 2004; Meibom et al., 2004; Walker et al., 2005). These grains either form from reduction and release of Os, Ir, and Ru following alteration of sulfides during serpentinization of peridotite, or are precipitates from magmas passing through the mantle lithosphere (Cabri and Harris, 1975; Peck and Keays, 1990; Brenker et al., 2003). Osmium-rich alloy grains have very low Re/Os and Pt/Os such that no measurable ingrowth of  $^{187}\text{Os}$  and  $^{186}\text{Os}$  occurs subsequent to their formation (Hattori and Hart, 1991; Walker et al., 1997; Bird et al., 1999; Meibom and Frei, 2002; Meibom et al., 2002; Brenker et al., 2003; Meibom et al., 2004; Walker et al., 2005). Therefore, these grains record the Os isotopic composition of their mantle source(s), and consequently, they should record the long-term Re/Os and Pt/Os of mantle precursors at the time of formation.

Previous work has shown that the present-day  $^{186}\text{Os}/^{188}\text{Os}$  of the Earth's upper mantle, as constrained by Os-rich alloys, abyssal peridotites, and chromites from ophiolites, is within uncertainties, similar to that of chondrites (Walker et al., 1997; Brandon et al., 1998; Brandon et al., 2000). The previously reported average  $^{186}\text{Os}/^{188}\text{Os}$  of the various upper mantle samples was  $0.1198365 \pm 0.0000055$  ( $2\sigma$ ), compared to  $0.1198310 \pm 0.0000060$  for

the CV3 chondrite Allende (Walker et al., 1997; Brandon et al., 2000). These results have demonstrated that the Earth's upper mantle has had a generally chondritic Pt/Os ratio over Earth history (Brandon et al., 2000). Recent analytical developments permit analysis of  $^{186}\text{Os}/^{188}\text{Os}$  to higher precision by a factor of approximately 3. This provides a reason to reexamine this isotopic ratio in both chondrites and mantle-derived materials to better constrain the long-term Pt/Os ratios of these materials. Here, we consider data for 28 Os-rich alloys from Phanerozoic peridotites (14 grains from Walker et al., 2005; 14 new grains). These data are compared with recently published data for 13 samples of carbonaceous, enstatite and ordinary chondrites (Brandon et al., 2005a). The chondrite data are used to refine the initial  $^{186}\text{Os}/^{188}\text{Os}$  of the solar system. The Os isotopic data for chondrites and the data for Os-rich alloys are then considered with respect to defining a primitive upper mantle growth curve. Finally, these data are used to constrain processes that may have affected the Os isotope and HSE budget of the upper mantle during early differentiation and during mantle evolution over Earth history.

## 2. Analytical techniques

The data for chondrites (Table 1) are from Brandon et al. (2005a,b). The Pt and Os concentrations were measured by isotope dilution-ICPMS following the techniques reported in Brandon et al. (2005a,b) and Horan et al. (2003). Where Pt and Os were not measured on the same aliquot, an additional uncertainty component was added using  $\pm 5\%$  ( $2\sigma$ ) on Pt/Os to the combined standard uncertainty for the initial  $^{186}\text{Os}/^{188}\text{Os}_i$  ratio at 4.567 Ga. This uncertainty is a worst-case scenario based on reproducibilities of Pt/Os on replicates of bulk chondrites from Brandon et al. (2005a,b) and Horan et al. (2003). On samples where Pt and Os were measured on the same aliquot, the uncertainty on Pt/Os is better than  $\pm 1\%$  and does not add significant uncertainty to the calculated  $^{186}\text{Os}/^{188}\text{Os}_i$  because of the very small  $^{190}\text{Pt}/^{188}\text{Os}$  and the large half-life of  $^{190}\text{Pt}$ . The two Allende fractions came from the same homogenized sample powder obtained from the Smithsonian Institution and the Pt/Os ratio for Fraction 1 is applied to both. All other replicates were processed from separate rock fragments.

All of the Os-rich alloys measured in this study (Table 2) were aliquots taken from Os cuts that were purified and measured in the earlier studies (Walker et al., 1997; Brandon et al., 1998; Meibom and Frei, 2002; Meibom et al., 2004; Walker et al., 2005) with the exception of Tasm-6 and Os Pellet. The latter two were obtained using techniques employed in Meibom et al. (2004).

Osmium isotopic compositions in all samples reported in Tables 1 and 2 were measured on a *ThermoElectron Triton* thermal ionization mass spectrometer in negative ion mode at the Johnson Space Center (JSC). The data were obtained

Table 1  
Osmium isotope data for chondrites (Brandon et al., 2005a)

Chondrites	$^{186}\text{Os}/^{188}\text{Os}$	$\pm 2\sigma$	Pt/Os	$^{190}\text{Pt}/^{188}\text{Os}$	$^{186}\text{Os}/^{188}\text{Os}_i^c$	$\pm 2\sigma$	$^{187}\text{Os}/^{188}\text{Os}$	$\pm 2\sigma$
Allende Fraction 1, CV3 (4)	0.1198351	0.0000007	1.811 <sup>a</sup>	0.001725	0.1198234	0.0000007	0.1260416	0.0000013
Allende Fraction 2	0.1198352	0.0000011			0.1198236	0.0000011	0.1262413	0.0000011
Tagish Lake Fraction KN2, C2 (3)	0.1198126	0.0000012	1.885 <sup>a</sup>	0.001795	0.1198005	0.0000012	0.1260697	0.0000020
Tagish Lake Fraction MCO1 1 (2)	0.1198072	0.0000023	2.082 <sup>a</sup>	0.001983	0.1197938	0.0000023	0.1266184	0.0000030
Tagish Lake Fraction MCO1 2 (4)	0.1198198	0.0000008			0.1198065	0.0000008	0.1271579	0.0000012
Tagish Lake Fraction MH11 (2)	0.1197953	0.0000011	1.975 <sup>a</sup>	0.001881	0.1197826	0.0000011	0.1260217	0.0000003
Ornans, CO3 (3)	0.1198304	0.0000009	1.963 <sup>a</sup>	0.001870	0.1198178	0.0000009	0.1264519	0.0000020
Sharps Fraction 1, H3.4 (5)	0.1198384	0.0000010			0.1198260	0.0000016	0.1283708	0.0000029
Sharps Fraction 2	0.1198387	0.0000016	1.920 <sup>a</sup>	0.001829	0.1198264	0.0000016	0.1283528	0.0000017
St. Marguerite, H4 (2)	0.1198392	0.0000010	2.073 <sup>a</sup>	0.001974	0.1198259	0.0000010	0.1292181	0.0000022
St. Marguerite Metal (6)	0.1198402	0.0000008	2.095 <sup>a</sup>	0.001995	0.1198267	0.0000008	0.1319446	0.0000015
Forest Vale, H4 (2)	0.1198401	0.0000006	1.936 <sup>b</sup>	0.001844	0.1198276	0.0000012	0.1287843	0.0000000
Weston, H5 (4)	0.1198408	0.0000009	2.037 <sup>a</sup>	0.001940	0.1198277	0.0000009	0.1302607	0.0000016
Allegan, H5 (4)	0.1198398	0.0000008	2.030 <sup>a</sup>	0.001933	0.1198268	0.0000008	0.1312607	0.0000025
Avg. H-Group Ordinary Chondrites	0.1198398	0.0000016 <sup>d</sup>	1.999	0.001903	0.1198269	0.0000014 <sup>d</sup>	0.12958	0.00105
Chainpur, LL3.4 (3)	0.1198368	0.0000011	1.914 <sup>b</sup>	0.001823	0.1198244	0.0000017	0.1289658	0.0000010
Parnellee, LL3.6 (3)	0.1198345	0.0000005	1.713 <sup>a</sup>	0.001631	0.1198235	0.0000005	0.1281180	0.0000013
Indarch Fraction 1, EH4 (3)	0.1198322	0.0000004			0.1198189	0.0000011	0.1282045	0.0000020
Indarch Fraction 2	0.1198348	0.0000010	2.060 <sup>a</sup>	0.001962	0.1198215	0.0000010	0.1281770	0.0000016
Yilmia Fraction 1, EL6 (5)	0.1198384	0.0000008			0.1198264	0.0000014	0.1275957	0.0000013
Yilmia Fraction 2	0.1198385	0.0000011	1.867 <sup>a</sup>	0.001778	0.1198265	0.0000011	0.1275762	0.0000013
Daniels Kuil, EL6 (2)	0.1198401	0.0000001	1.846 <sup>b</sup>	0.001758	0.1198282	0.0000007	0.1283851	0.0000007

Number of replicates for each datum is listed in parentheses.

<sup>a</sup> Data from Brandon et al. (2005a,b).

<sup>b</sup> Data from Horan et al. (2003).

<sup>c</sup>  $^{186}\text{Os}/^{188}\text{Os}_i$  are corrected to 4.567 Ga using present-day ratios and the Pt/Os ratios listed. The  $\pm 2\sigma$  uncertainties for these initial ratios include propagation of the Pt/Os ratio uncertainties. See the text and Brandon et al. (2005a) for further discussion.

<sup>d</sup> The  $\pm 2\sigma$  is for the averages of the present-day data and those corrected to initial at 4.567 Ga for H-group ordinary chondrites, respectively.

in static mode using 7 Faraday collectors. Signal intensities of 150–250 mV on mass 234 ( $^{186}\text{Os}^{16}\text{O}_3^-$ ) and 235 ( $^{187}\text{Os}^{16}\text{O}_3^-$ ) were generated for  $\geq 180$  ratios to reach the desired run precision of  $\pm 0.0000015$  or better ( $2\sigma_{\text{mean}}$ ) for the  $^{186}\text{Os}/^{188}\text{Os}$  ratio. Each cycle had an integration time of 17 s followed by a 4 s settling time. The isobaric interference of  $^{186}\text{W}^{16}\text{O}_3^-$  on  $^{186}\text{Os}^{16}\text{O}_3^-$  was monitored by measuring  $^{184}\text{Os}^{16}\text{O}_3^-$  ( $^{184}\text{W}^{16}\text{O}_3^-$ ). This interference has not been observed on the JSC Triton during Os measurements. Oxygen corrections were made using the oxygen isotopic composition obtained for 2 ng loads of  $\text{ReO}_4$  on the Faraday cups. Only one bottle of oxygen was used during the analytical campaign. Repeated measurements of the oxygen isotopic composition using Re indicated no change over time. The oxygen pressure for all runs was maintained in the range of  $2\text{--}3 \times 10^{-7}$  mbar. After oxygen corrections were made on the raw data, instrumental mass fractionation corrections were performed using the exponential law and  $^{192}\text{Os}/^{188}\text{Os} = 3.083$ . For all of the data reported in Tables 1 and 2, 1–8 replicate runs were made of each sample load and the average for each sample is reported with  $\pm 2\sigma_{\text{mean}}$ . The mean of 39 runs of the Johnson-Matthey Os standard during the analytical campaign was  $0.1198470 \pm 16$  for  $^{186}\text{Os}/^{188}\text{Os}$  and  $0.1137908 \pm 36$  for  $^{187}\text{Os}/^{188}\text{Os}$  ( $\pm 2\sigma$ ).

### 3. Discussion

#### 3.1. Pt–Os isotopic systematics of chondrites

Chondrite data (Table 1; Brandon et al., 2005a) were obtained with the same analytical protocol used to obtain data for Os-rich alloys during the same time interval using the Triton at JSC. These data were presented in Brandon et al. (2005a) using a normalization to  $^{192}\text{Os}/^{189}\text{Os}$  for the purpose of identifying s-process versus r-process presolar anomalies in the complete Os isotope mass spectrum. Here, the data are presented using the traditional normalization to  $^{192}\text{Os}/^{188}\text{Os}$  for direct comparison to terrestrial materials (Table 1). For the present study, the objective was to obtain precise  $^{186}\text{Os}/^{188}\text{Os}$  data for bulk chondrites that span a wide range of bulk major element compositions and petrologic types. Horan et al. (2003) reported only modest variability in Pt/Os among various types of meteorites with averages for carbonaceous, ordinary and enstatite chondrites of  $1.83 \pm 0.08$  ( $n = 12$ ),  $1.84 \pm 0.10$  ( $n = 12$ ), and  $1.87 \pm 0.08$  ( $n = 7$ ), respectively (all uncertainties  $\pm 2\sigma_{\text{mean}}$ ). The entire range of Pt/Os for the chondrites was 1.59–1.99, with the exception of an outlier of 1.37 for Ornans (CO3). Brandon et al. (2005a,b) reported a similar range in Pt/Os for all three chondrite groups ( $n = 13$ , Table 1) ranging

Table 2  
Osmium isotope data for Os-rich alloys

Os-rich alloys—SW Oregon <sup>a</sup>	<sup>186</sup> Os/ <sup>188</sup> Os	±2σ	<sup>187</sup> Os/ <sup>188</sup> Os	±2σ	T <sub>RD</sub> <sup>c</sup>
Matrix 1 (2)	0.1198403	0.0000002	0.1243534	0.0000028	0.72
Matrix 2 (2)	0.1198390	0.0000009	0.1245518	0.0000018	0.69
Matrix 3	0.1198352	0.0000025	0.1229181	0.0000025	0.92
Matrix 5 (3)	0.1198374	0.0000009	0.1274194	0.0000025	0.30
Matrix 6 (6)	0.1198393	0.0000009	0.1228888	0.0000008	0.92
Matrix 8 (2)	0.1198378	0.0000003	0.1261330	0.0000001	0.48
Lamellae 1 (3)	0.1198362	0.0000012	0.1227834	0.0000017	0.93
Lamellae 2 (2)	0.1198382	0.0000007	0.1222940	0.0000022	1.00
Lamellae 3 (2)	0.1198408	0.0000010	0.1468804	0.0000007	0.16
Lamellae 4 (3)	0.1198388	0.0000017	0.1314672	0.0000024	0.16
Lamellae 5 (6)	0.1198394	0.0000007	0.1412296	0.0000016	0.16
Lamellae 6 (3)	0.1198375	0.0000009	0.1295440	0.0000011	0.16
Lamellae 7 (3)	0.1198370	0.0000005	0.1207897	0.0000019	1.20
Lamellae 8	0.1198393	0.0000006	0.1209300	0.0000006	1.19
Os-rich alloys—various locations <sup>b</sup>					
AM 10-95—SW Oregon	0.1198398	0.0000010	0.1595461	0.0000013	0.16
AM 9-85-2—SW Oregon	0.1198377	0.0000012	0.1409429	0.0000013	0.16
AM 22-125—SW Oregon	0.1198369	0.0000011	0.1166746	0.0000011	1.76
PO 20—SW Oregon	0.1198320	0.0000013	0.1095268	0.0000012	2.71
Tasmania-6	0.1198360	0.0000010	0.1215616	0.0000011	1.10
Bald Hills	0.1198375	0.0000008	0.1200656	0.0000070	1.30
Yodda—Papua New Guinea	0.1198399	0.0000005	0.1290024	0.0000012	0.08
W5A (3)—unknown location	0.1198388	0.0000010	0.1242841	0.0000026	0.73
W5B (4)—unknown location	0.1198400	0.0000004	0.1242834	0.0000006	0.73
California (7)	0.1198390	0.0000008	0.1233602	0.0000008	0.86
Savage River (8)	0.1198382	0.0000009	0.1199733	0.0000008	1.32
19 Mile Creek (7)	0.1198370	0.0000010	0.1238699	0.0000012	0.79
Oregon (3)	0.1198376	0.0000003	0.1238042	0.0000006	0.80
Os Pellet—synthetic <sup>b</sup>	0.1198329	0.0000012	0.1096116	0.0000011	2.70

Number of replicates for each datum is listed in parentheses.

<sup>a</sup> Data from Walker et al. (2005).

<sup>b</sup> New data.

<sup>c</sup> T<sub>RD</sub> is the relative Re depletion age in Ga (Shirey and Walker, 1998, Eq. (5)), which is the time where it is assumed that all Re is removed from the Os-rich alloy mantle source during partial melting, or when the grains formed and were isolated from host mantle. See text for further explanation.

from 1.71 to 2.09. None of these studies show a systematic difference in the Pt/Os among the chondrite groups. This is not true for Re/Os which is distinctly lower, on average, in carbonaceous chondrites compared with ordinary or enstatite chondrites (Walker et al., 2002). The cause for the Re/Os bimodality remains unknown, but may relate to secondary processes on the parent bodies. The 50% condensation temperatures for Pt and Os are much more disparate than for Re and Os, so the modest variations in Pt/Os amongst individual chondrites likely reflect, in part, variations in the condensation temperatures of different components contained within each chondrite.

There is an additional complication in constraining the <sup>186</sup>Os/<sup>188</sup>Os, and hence, the long-term Pt/Os of chondrites.

Brandon et al. (2005a) showed that some chondrites contain what appear to be deficiencies in certain Os isotopes that form as a result of s-process nucleosynthesis (<sup>186</sup>Os, <sup>188</sup>Os, and <sup>190</sup>Os). Compared to H-chondrites, carbonaceous chondrites exhibit depletions in <sup>186</sup>Os and <sup>190</sup>Os, and some enstatite chondrites exhibit minor depletions in <sup>186</sup>Os. They concluded that the “missing” Os in these meteorites is likely present in presolar grains (SiC or diamond) that are insoluble in the acid digestion technique used for

dissolving samples and equilibrating spikes with samples. Their calculations showed that only a few parts per million of s-process Os of the total Os budget in a bulk chondrite, if not digested, will result in resolvable reduction in the <sup>186</sup>Os/<sup>188</sup>Os ratio of the processed material. Presolar SiC and other presolar grains are broken down with greater degrees of metamorphism within the different petrologic groups of chondrites (Huss and Lewis, 1995; Huss, 1997). Digestion of bulk chondrites with high metamorphic grades (e.g., 5 and 6) should therefore access Os that is potentially sited in insoluble presolar grains in unequilibrated chondrites of lower metamorphic grade. The efforts in this study are, therefore, directed towards equilibrated chondrites.

For the ordinary chondrites, samples examined in the H-group have metamorphic grades ranging from 3.4 (Sharps) to 5 (Allegan and Weston). These meteorites define a narrow range of <sup>186</sup>Os/<sup>188</sup>Os from 0.1198384 to 0.1198408 and calculated <sup>186</sup>Os/<sup>188</sup>Os<sub>i</sub> of 0.1198259–0.1198277. The averages for H-group chondrites for <sup>186</sup>Os/<sup>188</sup>Os and <sup>186</sup>Os/<sup>188</sup>Os<sub>i</sub> are 0.1198398 ± 0.0000016 and 0.1198269 ± 0.0000014 (2σ), respectively (Table 1 and Fig. 1). These uncertainties are similar to the long-term



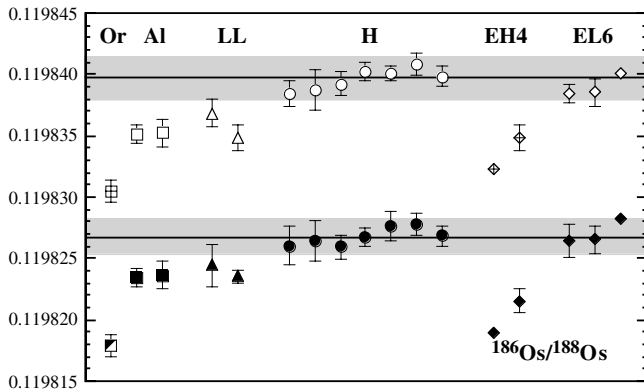


Fig. 1. The present-day  $^{186}\text{Os}/^{188}\text{Os}$  (open symbols) and  $^{186}\text{Os}/^{188}\text{Os}_i$  ratios at 4.567 Ga (solid symbols) for chondrites (Table 1; Brandon et al., 2005a). Abbreviations: Or, Ornaments; Al, Allende; LL, LL-group; H, H-group ordinary chondrites, and EH4 and EL6, enstatite chondrites. The lines and shaded regions are the averages and  $\pm 2\sigma$  error envelopes for H-group ordinary chondrites (Table 1), respectively. Errors bars are  $2\sigma$ . The correction to  $^{186}\text{Os}/^{188}\text{Os}_i$  for each chondrite is systematic at  $110 \pm 10$  ppm because of the near constant Pt/Os of  $1.9 \pm 0.2$  chondrites.

external precision of the standard of  $\pm 0.0000016$  and it can be concluded that these samples have unresolvable  $^{186}\text{Os}/^{188}\text{Os}$  and  $^{186}\text{Os}/^{188}\text{Os}_i$ .

### 3.2. Osmium-rich alloys

The majority of Os-rich alloy grains examined here were analyzed in previous studies (e.g., Walker et al., 1997; Brandon et al., 1998; Meibom and Frei, 2002; Meibom et al., 2004). The objective here was to reanalyze the Os cuts using the new higher precision measurement capabilities. Most of the grains considered here are from placer deposits collected downstream from the Josephine peridotite in SW Oregon (Table 2). Data for 14 of the grains were obtained using the new higher precision measurement capabilities and reported in Walker et al. (2005). These data are provided in Table 1 for completeness. Osmium isotopic compositions were obtained in this present study for four additional grains from this area that were provided by R. Frei (Geological Institute, University of Copenhagen). Analyses for these grains were previously published in Meibom and Frei (2002) and Meibom et al. (2004). These grains, along with a synthetic Os pellet, also obtained from Frei, additionally serve as useful points for interlaboratory comparison. In addition, the synthetic Os pellet provides a useful comparison of Os purified from an unknown source extracted from the mantle at some time in the past, and therefore likely represents an averaged mantle composition at that time. Finally, 9 of the grains sample ultramafic terrains from worldwide locations. Data for these grains were previously published in Walker et al. (1997) and Brandon et al. (1998), with the exception of Tasmania-6, which was supplied by R. Frei.

When the data from the different labs are normalized to a common  $^{186}\text{Os}/^{188}\text{Os}$  ratio for the Os standard used, the new, higher-precision measurements are in good agreement

with previous measurements (see also discussion in Walker et al., 2005), albeit with considerably reduced analytical uncertainties. The only major exception is grain AM-10-95 (Table 2) for which Meibom et al. (2004) reported a  $^{186}\text{Os}/^{188}\text{Os}$  of  $0.1198236 \pm 0.0000066$ . This ratio is 135 ppm lower than the  $^{186}\text{Os}/^{188}\text{Os}$  of  $0.1198398 \pm 0.0000010$  measured here. It should also be noted that Meibom et al. (2004) reported data for nine other grains, data for three of which are in good agreement with the new measurements in this present study. They also reported data for several grains that had considerably higher  $^{186}\text{Os}/^{188}\text{Os}$  ( $>0.119840$ ) than had previously been reported for Os-rich grains. Walker et al. (2005) discussed these results in the context of their data for 14 similar grains and concluded the higher ratios reported by Meibom et al. (2004) were likely analytical artifacts. The Os solutions for these grains were reportedly exhausted (Frei, personal communication, 2004), so it was not possible to reexamine these unusual grains here.

When all, new, high precision data for grains and the synthetic Os pellet are considered, they display a somewhat more restricted range in  $^{186}\text{Os}/^{188}\text{Os}$  than has been collectively reported by the previous studies (Fig. 2). The more limited scatter is consistent with the lower external precision for standards and samples of  $\pm 0.0000016$  ( $2\sigma$ ) established through repeated measurements. The more limited scatter allows a tighter constraint to be placed on the bulk  $^{186}\text{Os}/^{188}\text{Os}$  of the upper mantle than was possible with the results of previous studies. Nonetheless, despite the reduced scatter, there are resolvable differences in the  $^{186}\text{Os}/^{188}\text{Os}$  of the grains within the suite examined. For the new database, these resolvable differences of  $^{186}\text{Os}/^{188}\text{Os}$  between different grains record important information about the processes affecting HSE in the upper mantle. The new data will be considered in the following sections in the context of processes that may have fractionated Pt from Re and Os.

### 3.3. Origins of $^{186}\text{Os}/^{188}\text{Os}$ variations in the upper mantle

The Os-rich alloy grains have negligible Pt/Os and Re/Os ratios, such that their measured  $^{186}\text{Os}/^{188}\text{Os}$  and  $^{187}\text{Os}/^{188}\text{Os}$  ratios record the composition of their host material (i.e., the mantle or magmatic parent) at the time of their crystallization. With the exception of two samples that have  $^{186}\text{Os}/^{188}\text{Os} < 0.0119835$ , all of the Os-rich alloys measured in this study overlap the range of  $^{186}\text{Os}/^{188}\text{Os}$  for ordinary chondrites (Fig. 3). Of particular note, the maximum  $^{186}\text{Os}/^{188}\text{Os}$  of  $0.1198408 \pm 0.0000010$  and the average  $^{186}\text{Os}/^{188}\text{Os}$  of  $0.1198382 \pm 0.0000028$  ( $2\sigma$ ,  $n = 26$ ) overlap with the average for the five H-group chondrites of  $0.1198398 \pm 0.0000016$  ( $2\sigma$ ,  $n = 5$ ), and also the average for three equilibrated enstatite chondrites of  $0.1198408 \pm 0.0000009$  reported by Brandon et al. (2005a). The most straightforward explanation for the systematics is that the primitive upper mantle has evolved over time with a Pt/Os ratio, and had an initial  $^{186}\text{Os}/^{188}\text{Os}$  ratio that is

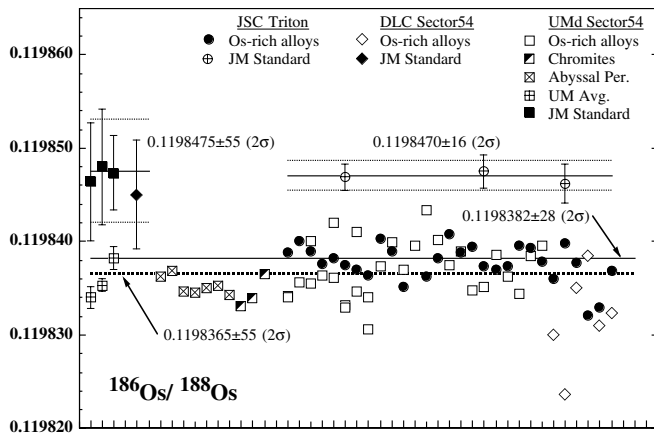


Fig. 2. A comparison of the present-day  $^{186}\text{Os}/^{188}\text{Os}$  ratios for the Johnson-Matthey (JM) standard and upper mantle materials measured by TIMS at JSC (Johnson Space Center), DLC (Danish Lithosphere Center), and UMD (University of Maryland). Values obtained for the averages and error bars ( $\pm 2\sigma$ ) for replicates of the JM standard over different time intervals are shown for the three instruments. The long-term  $^{186}\text{Os}/^{188}\text{Os}$  of the mean with corresponding  $\pm 2\sigma$  error at UMD for the JM standard of  $0.1198475 \pm 55$  is shown by a solid line and dashed lines, respectively, as is the long-term  $^{186}\text{Os}/^{188}\text{Os}$  of the mean on the Triton of  $0.1198470 \pm 16$ . The sample data shown typically have errors of  $\pm 0.000005$  ( $2\sigma$ ) or better for the Sector 54 at both DLC and UMD, and  $\pm 0.000002$  ( $2\sigma$ ) or better for the Triton at JSC. Replicates for individual samples on the Triton versus the Sector 54 at DLC or UMD, are plotted vertically relative to each other on the same  $x$ -axis tick mark. For samples measured at UMD, upper mantle averages (UM Avg.) obtained on different sample suites are shown, with a combined average for all of the samples shown as a dashed line with  $^{186}\text{Os}/^{188}\text{Os} = 0.1198365 \pm 55$  ( $2\sigma$ ). The samples suites included Os-rich alloys, chromites from ophiolites, and Kane Fracture Zone abyssal peridotites (Abyssal Per.). The average for all Os-rich alloys measured on the Triton is shown by a solid line with  $^{186}\text{Os}/^{188}\text{Os} = 0.1198382 \pm 28$  ( $2\sigma$ ).

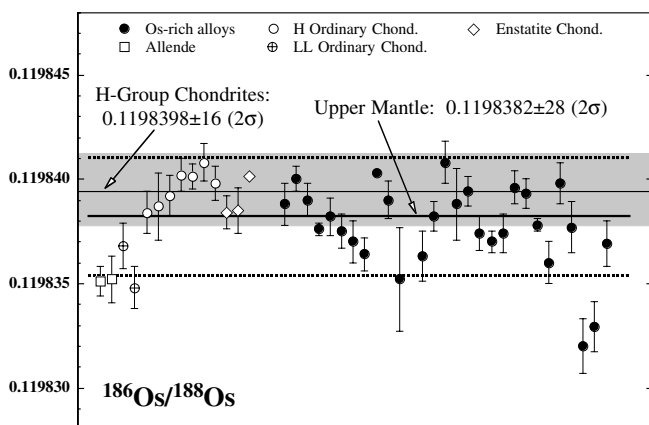


Fig. 3. The present-day  $^{186}\text{Os}/^{188}\text{Os}$  of Os-rich alloy samples and chondrites measured on the Triton. Error bars are  $\pm 2\sigma$ . Chondrite data that may result from incomplete access of Os retained in acid resistant presolar grains are not shown. See text for discussion on this issue. The average for H-group chondrites is shown by a thin solid line, and the  $\pm 2\sigma$  error envelope is shown by the shaded region. The average and  $\pm 2\sigma$  error for the upper mantle represented by these Os-rich alloy data is shown by a thick solid line and dashed lines, respectively.

unresolvable from H-group and equilibrated E-group chondrites. This explanation will be further tested in the following discussion.

Several of the Os-rich alloy samples have  $^{186}\text{Os}/^{188}\text{Os}$  ratios that are lower than ordinary H-group chondrites (Fig. 3). These lower ratios can be explained by any one of at least three possible scenarios, each with its own set of unique implications for upper mantle dynamics. For scenario 1, the mantle sources for these  $^{186}\text{Os}$ -depleted samples could have evolved from the time of early differentiation with Pt/Os ratios that are lower than H-group chondrites. If data for the LL-group chondrites and Allende are representative of their bulk values (a matter discussed above and at present not known), and if a late veneer following core formation controlled the HSE budget of the upper mantle during early differentiation (Morgan, 1986; Morgan et al., 2001), then the lower  $^{186}\text{Os}/^{188}\text{Os}$  ratios for some of the Os-rich alloys may have resulted from compositional variation in accreted materials. In this case, convective mixing of the mantle since early differentiation has not been efficient enough to homogenize these initial heterogeneities in HSE at the very small length scales of approximately 1 m, constrained by the volume of mantle necessary ( $1 \text{ m}^3$ ) to derive enough Os contained in an average Os-rich alloy grain (Meibom et al., 2002; Walker et al., 2005).

For scenario 2, it is envisioned that it is the grains with the lowest  $^{186}\text{Os}/^{188}\text{Os}$  that define the present composition of the evolving upper mantle, and that the grains with higher  $^{186}\text{Os}/^{188}\text{Os}$  reflect addition of Os-bearing materials into upper mantle with higher time-integrated Pt/Os ratios. One possible source of high Pt/Os material is an evolving outer core, which could be mixed into mantle sources through core–mantle interaction (Walker et al., 1995, 1997; Brandon et al., 1998, 1999b, 2003; Bird et al., 1999; Meibom and Frei, 2002; Brandon and Walker, 2005). A long-term high Pt/Os in the outer core would result in an elevated  $^{186}\text{Os}/^{188}\text{Os}$  during the Phanerozoic when the Os-rich alloy grains formed. Models for core evolution suggest that the present-day  $^{186}\text{Os}/^{188}\text{Os}$  for the evolved outer core could be as high as 0.119870 (Brandon et al., 2003). If the higher  $^{186}\text{Os}/^{188}\text{Os}$  for the Os-rich grains are the result of core–mantle interaction, then the fact that most of the grains examined have this enriched signal means that such a process is pervasive over large regions of the mantle. This would have important ramifications for dynamic models of mantle mixing.

For scenario 3, it is assumed that most Os-rich grains originated in ambient mantle that at one time evolved with a Pt/Os consistent with the H-chondrites. Depleted  $^{186}\text{Os}/^{188}\text{Os}$  in some grains could result from: (1) a combination of ancient mantle melt depletion, leading to a lowering of Pt/Os (i.e.,  $D_{\text{Os}} > 1$ ,  $D_{\text{Pt}} < 1$ , Puchtel and Humayun, 2000; Puchtel et al., 2004b), and consequent retardation in the growth of  $^{186}\text{Os}/^{188}\text{Os}$  in the residual mantle, followed by grain formation in the residual mantle at a time subsequent to the depletion event, or (2) direct formation of grains with very low Pt/Os from the evolving ambient mantle at some time in the distant past, followed by subsequent isolation of the grains until sampled.

Formation of mantle with sufficiently depleted Pt/Os to account for some of the lower  $^{186}\text{Os}/^{188}\text{Os}$  values can be generated only if the depletion occurred long ago and resulted from large degrees of partial melting. Such melting would normally lead to the production of komatiitic lavas, rather than basaltic. A lowering of Pt/Os can be achieved in this manner because, for large degrees of melting, Pt has a  $D$  of  $\sim 0.1$ – $0.5$  while Os has a  $D \sim 2$  (Puchtel and Humayun, 2000; Puchtel et al., 2004b). Consequently, melt removal will lead to formation of residue with moderately reduced Pt/Os compared to the fertile mantle. If Os isotope data for the samples are explained by this, then the implication is that depleted grains formed from material residual to Archean komatiite production.

Depleted grains could also simply have formed at some time in the past and evolved to the present with little or no subsequent increase in  $^{186}\text{Os}/^{188}\text{Os}$ . The implication here is that some of these grains can survive in the mantle for several Ga. The differences in  $^{186}\text{Os}/^{188}\text{Os}$  among the suite examined would then reflect different formation ages for the grains.

Critical to assessing these possibilities is the Re–Os isotope system. Rhenium is incompatible during partial melting while Os is compatible (Walker et al., 1988, 1989, 1999; Hauri and Hart, 1997), so residual mantle, such as that occurring as subcontinental lithospheric mantle, tends to have  $^{187}\text{Os}/^{188}\text{Os}$  that reflect the minimum times of partial melting of the mantle sources. Isolation of the Os-rich alloy grains from their mantle sources in the third scenario would cause retardation in the growth of both  $^{186}\text{Os}/^{188}\text{Os}$  and  $^{187}\text{Os}/^{188}\text{Os}$  because of the very low Pt/Os and accompanying Re/Os of Os-rich grains (Walker et al., 2005). This would result in preservation of the time of formation in the  $^{187}\text{Os}/^{188}\text{Os}$  (Malitch, 2004; Walker et al., 2005). Hence, the time of Re depletion ( $T_{\text{RD}}$  model age, Shirey and Walker, 1998) can be calculated and used to constrain whether scenario 3 can explain the observed variations in  $^{186}\text{Os}/^{188}\text{Os}$  among the Os-rich alloy grains.

The  $T_{\text{RD}}$  model ages in Ga (Table 2) are calculated relative to the present-day PUM where  $^{187}\text{Os}/^{188}\text{Os} = 0.1296 \pm 0.0008$  and  $^{187}\text{Re}/^{188}\text{Os} = 0.4346$  (Meisel et al., 2001), using Eq. (5) of Shirey and Walker (1998). For six samples from SW Oregon with  $^{187}\text{Os}/^{188}\text{Os} > 0.1284$ , which is PUM at 162 Ma (i.e., the age of the host ophiolite, Walker et al., 2005), the  $T_{\text{RD}}$  ages are younger than the host (and grains give future ages). Instead, an age of 0.16 Ga is assigned for these samples (Table 2). This is the youngest possible age for the formation of these grains. All others have  $T_{\text{RD}}$  ages that are greater or equal to the ages of their host ophiolites. The  $T_{\text{RD}}$  ages range from 0.08 to 2.71. Using these ages as the assumed times of Re removal, the  $^{186}\text{Os}/^{188}\text{Os}$  of each grain is plotted on a Pt/Os evolution diagram (Fig. 4). All data plot within analytical uncertainties of the Pt/Os evolution curve for H-group chondrites, assuming the  $2\sigma$  uncertainties previously defined for the curve, and the appropriate uncertainties for each sample. These systematics indicate that ancient melt depletion or

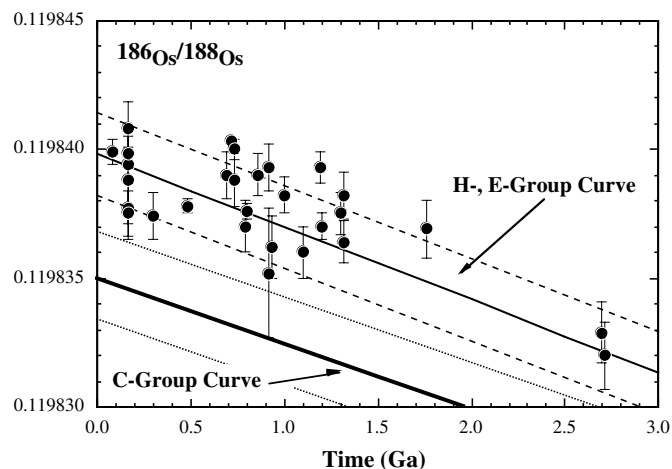


Fig. 4. The  $^{186}\text{Os}/^{188}\text{Os}$  versus time for the Os-rich alloy data. The  $^{186}\text{Os}/^{188}\text{Os}$  data for the Os-rich alloys are plotted versus TRD ages calculated from their respective  $^{187}\text{Os}/^{188}\text{Os}$  ratios. The proposed  $^{186}\text{Os}/^{188}\text{Os}$ -time evolution curve for the upper mantle (H-, E-Group Curve) and the carbonaceous chondrite time evolution curve (based on Allende data) are shown as solid lines with respective  $\pm 2\sigma$  errors shown as dashed lines.

grain formation from ambient mantle best explains the new data. Neither heterogeneities that remain from early Earth differentiation processes (scenario 1) nor pervasive, long-term core–mantle interaction (scenario 2) can as satisfactorily account for the coupled depletions in  $^{186}\text{Os}$  and  $^{187}\text{Os}$ , although neither possibility can be completely ruled out at this time for individual grains.

### 3.4. Effects of melt-enrichment processes

Several of the Os-rich grains have  $^{187}\text{Os}/^{188}\text{Os}$  that are enriched relative to the ambient upper mantle (e.g., samples range to as high as 0.1595), but have  $^{186}\text{Os}/^{188}\text{Os}$  that are not anomalously high (Fig. 5). Such high  $^{187}\text{Os}/^{188}\text{Os}$  cannot result from the processes discussed above. Previous studies have considered melt enrichment processes, especially as related to subduction zones, where crustal portions of slabs have strongly radiogenic  $^{187}\text{Os}/^{188}\text{Os}$ , as a means of causing  $^{187}\text{Os}$  enrichments in peridotites and Os-rich grains (Brandon et al., 1996, 1999a; McInnes et al., 1999; Peslier et al., 2000; Becker et al., 2001, 2004; Widom et al., 2003). This is an important aspect of Os evolution to consider for this study, because melt enrichment could potentially also lead to  $^{186}\text{Os}/^{188}\text{Os}$  that is not representative of the bulk upper mantle.

Partial melts and their crustal derivatives typically evolve to very high  $^{187}\text{Os}/^{188}\text{Os}$  and possibly  $^{186}\text{Os}/^{188}\text{Os}$ , but have subchondritic Pt/Re. Thus, they evolve along  $^{186}\text{Os}/^{188}\text{Os}$  versus  $^{187}\text{Os}/^{188}\text{Os}$  trajectories that are shallower than that for upper mantle growth curve (Fig. 5; Brandon et al., 1998, 1999b). Hence, the anticipated consequence of melt-enrichment of a mantle reservoir is to produce hybrid mantle that evolves to  $^{187}\text{Os}/^{188}\text{Os}$  that is higher than the ambient mantle, but leads to little change



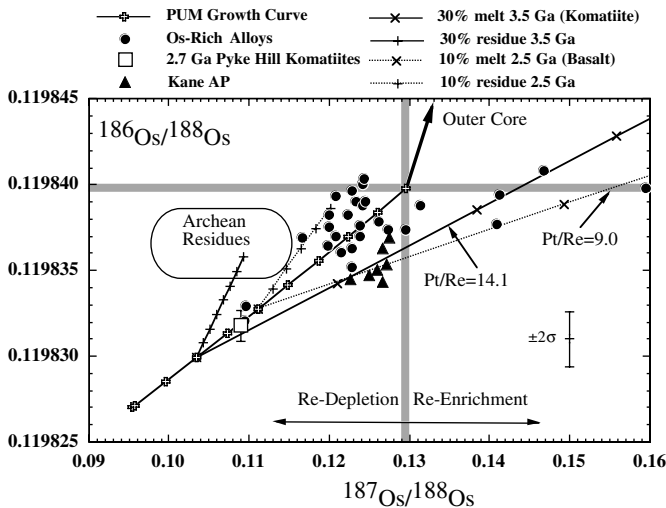


Fig. 5. The  $^{187}\text{Os}/^{188}\text{Os}$  versus  $^{186}\text{Os}/^{188}\text{Os}$  data for the Os-rich alloys, the 2.7 Ga Pyke Hill komatiites with  $\pm 2\sigma$  error bar (Puchtel et al., 2004a), and the Kane Fracture Zone abyssal peridotites (AP) from Brandon et al. (2000). The primitive upper mantle (PUM) growth curve evolves from 4.567 Ga assuming the Pt/Os systematics for the average of H-group ordinary chondrites and the Re/Os systematics proposed for PUM by Meisel et al. (1996, 2001). The evolution lines for 30% partial melting to produce komatiite melt (i.e., 30% melt) and residue (i.e., 30% residue) from 3.5 Ga to present were calculated for batch melting at 3.5 Ga using  $D_{\text{Os}} = 2.12$ ,  $D_{\text{Pt}} = 0.41$  (Puchtel and Humayun, 2000), and  $D_{\text{Re}} = 0.1$  (Hauri and Hart, 1997). The starting composition has a Pt/Os = 2.0, Re/Os = 0.0896, and Pt/Re = 22.31. Following melting, the residue has Pt/Os = 1.18, Re/Os = 0.0204, and Pt/Re = 57.8, while the komatiite melt has Pt/Os = 6.08, Re/Os = 0.4321, and Pt/Re = 14.1. The evolution lines for 10% partial melting to produce basalt melt (i.e., 10% melt) and residue (i.e., 10% residue) at 2.5 Ga to present were calculated for batch melting at 2.5 Ga using the same  $D$ 's as in the 30% partial melting with the same starting Pt/Os and Re/Os. Following melting, the residue has Pt/Os = 1.65, Re/Os = 0.0447, and Pt/Re = 36.9, while the basalt melt has Pt/Os = 8.56, Re/Os = 0.9470, and Pt/Re = 9.0. The plus and cross marks on each evolution line are at 500 Ma time intervals. The typical  $2\sigma$  uncertainty for the data are shown by the error bar on the right side of the diagram. The field for residues of partial melting in the Archean using the models calculated here is shown. A vector for mixing between PUM and hypothetical evolved outer core (Brandon et al., 1999b, 2003) is shown.

in  $^{186}\text{Os}/^{188}\text{Os}$ . These relationships indicate that although melt enrichment may have played a major role in the generation of the high  $^{187}\text{Os}/^{188}\text{Os}$  of some grains, this process would have had no resolvable effect on  $^{186}\text{Os}/^{188}\text{Os}$ .

Rhenium-enrichment with little or no Pt-enrichment in the mantle is not only restricted to subduction zone settings. Recent evidence has shown that abyssal peridotites from the Kane Fracture Zone in the Atlantic Ocean have interacted with melts that are enriched in  $^{187}\text{Os}/^{188}\text{Os}$  (Alard et al., 2005). These melts must come from sources that have long-term Re/Os enrichment. Brandon et al. (2000) considered melt-rock reaction for Kane abyssal peridotites and reported that correlations between Pt/Os (from 1.5 to 2.2) and  $^{187}\text{Os}/^{188}\text{Os}$  (from 0.1227 to 0.1276) could be explained by such a model only if the melts had  $^{187}\text{Os}/^{188}\text{Os}$  that were  $>0.13$ , consistent with the later findings by Alard et al. (2005). The samples examined by Brandon et al. (2000) have a restricted range in  $^{186}\text{Os}/^{188}\text{Os}$  from

$0.1198343 \pm 0.0000041$  to  $0.1198369 \pm 0.0000014$ . The average  $^{186}\text{Os}/^{188}\text{Os}$  for these samples is  $0.1198353 \pm 0.0000018$  ( $n = 7$ ,  $2\sigma$ ). All of the samples plot to the right of the upper mantle growth curve defined by H-group chondrites (Fig. 5). Since no resolvable differences in  $^{186}\text{Os}/^{188}\text{Os}$  are present in these samples, then the enrichment in  $^{187}\text{Os}/^{188}\text{Os}$  must have resulted from interaction with melts that were derived from sources with no long-term enrichment in Pt/Os.

### 3.5. Implications for core–mantle interaction

Mantle-derived samples of three Phanerozoic systems show coupled enrichments in  $^{186}\text{Os}/^{188}\text{Os}$  and  $^{187}\text{Os}/^{188}\text{Os}$  at the time of their formation. These systems are: (1) essentially modern picrites from Hawaii, (2) a picrite-derived sample from the ca. 251 Ma Siberian plume, and (3) komatiites from the 89 Ma Gorgona Island, Colombia (Walker et al., 1997; Brandon et al., 1998, 1999b, 2003). All three systems formed from magmas with high Os concentrations that would have been insensitive to crustal contamination. Hence, the coupled enrichments must be characteristic of their mantle sources. The mantle sources, in turn, must have been characterized by long-term suprachondritic Pt/Re of about 90, as compared to chondritic upper mantle with Pt/Re of 22 (Brandon et al., 1999b, 2003). The high Pt/Re, Pt/Os, and Re/Os necessary to produce the coupled enrichments in  $^{186}\text{Os}/^{188}\text{Os}$  and  $^{187}\text{Os}/^{188}\text{Os}$  is thought to be the result or addition of evolved outer core into the mantle sources for these materials (Walker et al., 1997; Brandon et al., 1998, 1999b, 2003). This is because in Fe-rich metal systems the solid metal/liquid metal partition coefficients are  $\text{Pt} < \text{Re} < \text{Os}$ , leading to higher Pt/Re, Pt/Os, and Re/Os in the evolved liquid (Walker et al., 1995) and over time will result in an evolved outer core with coupled enrichments in  $^{186}\text{Os}/^{188}\text{Os}$  and  $^{187}\text{Os}/^{188}\text{Os}$ .

Komatiite and basalt melts generally have subchondritic Pt/Re ratios of 14 or less (Fig. 5), and mantle sources that have undergone melt-enrichment result in evolution trajectories that are shallower than observed for the Hawaiian, Gorgona, and Siberia data. As discussed above, the Re–Os and Pt–Os isotope systematics of the Os-rich alloys, in combination with Pyke Hill komatiites (Puchtel et al., 2004a), and abyssal peridotites from the Kane fracture zone (Brandon et al., 2000), show no evidence for pervasive, long-term addition of evolved outer core material into the convecting mantle (Fig. 5). These constraints imply that coupled enrichments of  $^{186}\text{Os}/^{188}\text{Os}$  and  $^{187}\text{Os}/^{188}\text{Os}$  are restricted to plume systems. Enrichment processes in most of the convecting upper mantle that may occur in subduction zone settings or at mid-ocean ridges, results in elevated  $^{187}\text{Os}/^{188}\text{Os}$  without resolvable increases in  $^{186}\text{Os}/^{188}\text{Os}$ .

These observations are consistent with two possible scenarios for the impact of core–mantle interaction on the convecting upper mantle. In the first scenario, if core–mantle interaction occurs at the base of the mantle, the process is very localized such that only a small fraction of plume



sources are affected, resulting in minimal impact on the composition of the HSE budget of the convecting mantle. This scenario is consistent with the fact that only a portion of the samples analyzed from any plume system show coupled enrichments of  $^{186}\text{Os}/^{188}\text{Os}$  and  $^{187}\text{Os}/^{188}\text{Os}$  that are greater than the upper mantle values defined by the Os-rich alloy data presented here (Walker et al., 1997; Brandon et al., 1998; Brandon et al., 1999b; Brandon et al., 2003). In a second scenario, enrichment in HSE in the mantle from core–mantle interaction occurred early enough such that the  $^{186}\text{Os}/^{188}\text{Os}$  and  $^{187}\text{Os}/^{188}\text{Os}$  of the evolving outer core were not different from those of the convecting upper mantle. In this scenario, part or all of the HSE budget of the convecting mantle could be the result of pervasive core–mantle interaction in the early Archean. For the anticipated amount of core addition ( $\sim 0.5\%$ , Brandon and Walker, 2005), the process resulted in no resolvable increase in Os isotope ratios for the mantle source. For the second scenario to be valid, the early outer core would have chondritic relative proportions of HSE, consistent with the observed chondritic abundance ratios in mantle peridotite (Morgan et al., 2001). Recent core evolution models that purport to explain small coupled enrichments of  $^{186}\text{Os}/^{188}\text{Os}$  ( $\sim 20$  ppm) and  $^{187}\text{Os}/^{188}\text{Os}$  ( $\sim 2.5\%$ ) for the 2.8 Ga Kostomuksha komatiites, suggest that the inner core began to crystallize no later than 3.0 Ga (Puchtel et al., 2005). Hence, the Pt/Os and Re/Os ratios of the evolving outer core during the early Archean, would have been chondritic or nearly so prior to this time, and the HSE data for upper mantle peridotites are consistent with an early core replenishment model for explaining the HSE abundances of the upper mantle. A process proposed by Rushmer et al. (2005), where impact-driven, stress-induced dilatancy drives bulk core fluid back into the mantles of small planetesimals, may have operated early in solar system history. Whether this process or another as yet defined process can apply to large planets is at present unconstrained. This scenario will require additional examination using independent constraints from those presented here, including a better understanding of the thermal evolution of the Earth and how this impacts the onset of inner core formation.

### 3.6. Late Veneer versus metal–silicate equilibrium

Segregation of the metal-rich core resulted in strong depletion of HSE in the silicate portion of Earth. However, mantle-derived peridotites have concentrations of HSE that are orders of magnitude too high to be explained by core segregation at low pressures (Chou, 1978; Morgan et al., 1981; Morgan, 1986). As noted earlier, ratios between the HSE are generally chondritic in mantle peridotites. These observations have led to several hypotheses that attempted to explain the HSE concentrations in the Earth's mantle, including outer core liquid metal flux back into the convecting mantle during the early Archean, considered in the previous section. Two other additional end-

member models have received the most attention. In the first model, the HSE were replenished in the silicate Earth by a chondritic late veneer (i.e., the last  $\leq 1\%$  of planetary accretion) that followed core metal segregation (Chou, 1978; Morgan et al., 1981; Morgan, 1986). This model has merit in that it can adequately explain the observation of chondritic HSE ratios in mantle peridotites, and the fact that only a very small amount of late accretion following core segregation is necessary to explain the HSE concentrations. A second model proposes that liquid metal segregation took place at the base of a magma ocean that existed to mid-mantle depths. The higher temperatures and/or pressures may result in much lower metal–silicate distribution coefficients (e.g., Murthy, 1991). This model has been quite successful in explaining moderately siderophile element abundances in the mantle (Righter et al., 1997; Righter, 2003). Also, using metal liquid/silicate liquid partition coefficients for Re and Au obtained for these conditions in the mantle (Righter and Drake, 1997; Danielson et al., 2005), the concentrations of these two elements in mantle peridotites can potentially be explained by such a model obviating the need for a late veneer to replenish the HSE. Hence, both of these models have appeal within the present constraints of HSE behavior in metal and silicate systems.

The combined  $^{186}\text{Os}/^{188}\text{Os}$  and  $^{187}\text{Os}/^{188}\text{Os}$  data for the Os-rich alloys are most readily explained as a result of evolution from a mantle source with Pt–Re–Os isotope systematics that were similar to H-group chondrites (Figs. 4 and 5). Such a model can be explained via a late veneer of material averaging this composition following core separation (Meisel et al., 1996; Brandon et al., 2000; Morgan et al., 2001). The high-pressure metal segregation model would require very similar metal–silicate partitioning of Pt, Re, and Os during metal segregation such that virtually no fractionation in Pt/Os and Re/Os could have occurred. Recent experiments show that high-pressure metal–silicate bulk distribution coefficients ( $D$  values) between different HSE vary by orders of magnitude, such that it is unlikely that such a process can account for the precisely chondritic Pt/Os and Re/Os of PUM (Walker et al., 1997; Holzheid et al., 2000). However, these constraints do not completely rule out that metal–silicate equilibrium during core extraction at mid-mantle depths produced the observed HSE abundances in the upper mantle (Righter and Drake, 1997; Danielson et al., 2005). The primary caveat for this model is that the metal–silicate  $D$  values for all HSE must be within a factor of two or closer to explain the observed chondritic HSE abundances. From the perspective of the Pt/Os isotopic system, the fact that almost all of the Os-rich alloys and Pyke Hill komatiites plot within uncertainty of the proposed primitive upper mantle growth curve (Fig. 4), means that the Pt and Os partition coefficients must have been even more similar in value if a metal–silicate equilibrium model applies to the HSE abundances of the upper mantle. The Os-rich alloy and 2.7 Ga Pyke Hill komatiite data fall within  $\pm 0.0000016$  ( $2\sigma$ ) of the  $^{186}\text{Os}/^{188}\text{Os}$  PUM evolution curve defined by H-group

chondrites (Figs. 4 and 5) with a Pt/Os ratio of 2 (Table 1). This variation in  $^{186}\text{Os}/^{188}\text{Os}$  corresponds to a deviation of no more than  $\pm 10\%$  from the H-group chondrite Pt/Os ratio (i.e., Pt/Os =  $2.0 \pm 0.2$ ). Hence, these data provide the most precise measure of the values required for HSE partition coefficients during core extraction. Any core separation model must be able to explain this chondritic initial Pt/Os ratio for a starting bulk upper mantle composition if it is to be considered applicable.

#### 4. Conclusions

The best estimate for the  $^{186}\text{Os}/^{188}\text{Os}$  of the bulk solar system values is obtained from H-group chondrites, which have present-day  $^{186}\text{Os}/^{188}\text{Os} = 0.1198398 \pm 0.0000016$ , and  $^{186}\text{Os}/^{188}\text{Os}_i = 0.1198269 \pm 0.0000014$ . This corresponds to a Pt/Os =  $2.0 \pm 0.2$  for the PUM evolution curve. The  $^{186}\text{Os}/^{188}\text{Os}$  data for mantle-derived Os-rich alloys are consistent with these grains being derived from the Proterozoic to Phanerozoic convecting upper mantle that evolved with Pt/Os isotope systematics that are indistinguishable from H-group (and enstatite chondrites). Melt removal has had little impact on the Pt/Os of the convecting upper mantle during Earth history because of the similar  $D$  values for Pt and Os for relatively low extents of partial melting.

The  $^{186}\text{Os}/^{188}\text{Os}$  and  $^{187}\text{Os}/^{188}\text{Os}$  data for the Os-rich alloys indicate that the primary mechanisms for melt enrichment in the convecting upper mantle result in no increase in  $^{186}\text{Os}/^{188}\text{Os}$  with strong increases in  $^{187}\text{Os}/^{188}\text{Os}$ . This is in contrast to the coupled enrichments in  $^{186}\text{Os}/^{188}\text{Os}$  and  $^{187}\text{Os}/^{188}\text{Os}$  for some samples in plume systems. The systematics indicate that the different materials show two different styles of  $^{187}\text{Os}$  isotope enrichments. For samples from subduction zones and mid-ocean ridges, the sources of  $^{187}\text{Os}$  are likely crustal in origin characterized by subchondritic Pt/Re ratios and very high Re/Os. For samples that show coupled enrichments in  $^{186}\text{Os}/^{188}\text{Os}$  and  $^{187}\text{Os}/^{188}\text{Os}$ , a source with suprachondritic Pt/Re, Pt/Os, and Re/Os is necessary. Samples with these Os isotope systematics are known only to be present in some putative plume systems. To date, the only potential source that has been postulated to have these characteristics, that would be pervasive and isotopically homogeneous, and could be accessed in mantle sources from widely dispersed locales, is the outer core.

The Os isotope systematics of the Os-rich alloys are consistent with a model where core–mantle interaction has had little effect on the overall HSE budget in the mantle, unless it occurred very early in Earth history prior to when the outer core began to develop strong enrichments in Pt/Os and Re/Os, with consequent evolution to higher  $^{186}\text{Os}/^{188}\text{Os}$  and  $^{187}\text{Os}/^{188}\text{Os}$ , respectively. The alternative mechanism to create the observed  $^{186}\text{Os}/^{188}\text{Os}$  and  $^{187}\text{Os}/^{188}\text{Os}$  compositions is post-core-formation replenishment of HSE via late accretion. To determine which of these scenarios operated, additional investigation will be required.

#### Acknowledgments

This work was supported by NASA Grants to A.D.B. (RTOP 344-31-72-06) and R.J.W. (NNG04GK52G), NSF Grant (EAR0330528) to R.J.W., and by NSF Grants (EAR-0309786, EAR-0509176) to I.S.P. We thank Robert Frei for sending Os cuts of six Os-rich alloy solutions previously analyzed at the Danish Lithosphere Center. We thank Munir Humayun for his insights provided for this work. We thank Ambre Luguët, Monica Handler, and an anonymous person for their constructive journal reviews. Martin Menzies is thanked for editorial handling.

Associate editor: Martin A. Menzies

#### References

- Alard, O., Luguët, A., Pearson, N.J., Griffin, W.L., Lorand, J.-P., Gannoun, A., Burton, K.W., O'Reilly, S.Y., 2005. In situ Os isotopes in abyssal peridotites bridge the isotopic gap between MORBs and their source mantle. *Nature* **436**, 1005–1008.
- Bird, J.M., Meibom, A., Frei, R., Nagler, T.F., 1999. Osmium and lead isotopes of rare OsIrRu minerals: derivation from the core–mantle boundary region? *Earth Planet. Sci. Lett.* **170**, 83–92.
- Becker, H., Carlson, R.W., Shirey, S.B., 2004. Slab-derived osmium and isotopic disequilibrium in garnet pyroxenites from a Paleozoic convergent plate margin (lower Austria). *Chem. Geol.* **208**, 141–156.
- Becker, H., Shirey, S.B., Carlson, R.W., 2001. Effects of melt percolation on the Re–Os systematics from a Paleozoic convergent plate margin. *Earth Planet. Sci. Lett.* **188**, 107–121.
- Begemann, F., Ludwig, K.R., Lugmair, G.W., Min, K., Nyquist, L.E., Patchett, P.J., Renne, P.R., Shih, C.-Y., Villa, I.M., Walker, R.J., 2001. Call for an improved set of decay constants for geochronological use. *Geochim. Cosmochim. Acta* **65**, 111–121.
- Brandon, A.D., Creaser, R.A., Shirey, S.B., Carlson, R.W., 1996. Osmium recycling in subduction zones. *Science* **272**, 861–864.
- Brandon, A.D., Becker, H., Carlson, R.W., Shirey, S.B., 1999a. Isotopic constraints on time scales and mechanisms of slab material transport in the mantle wedge: evidence from the Simcoe mantle xenoliths, Washington, USA. *Chem. Geol.* **160**, 387–407.
- Brandon, A.D., Humayun, M., Puchtel, I.S., Leya, I., Zolensky, M., 2005a. Osmium isotope evidence for an s-process carrier in primitive chondrites. *Science* **309**, 1233–1236.
- Brandon, A.D., Humayun, M., Puchtel, I.S., Zolensky, M., 2005b. Re–Os isotopic systematics and platinum group element concentration of the Tagish Lake carbonaceous chondrite. *Geochim. Cosmochim. Acta* **69**, 1619–1631.
- Brandon, A.D., Norman, M.D., Walker, R.J., Morgan, J.W., 1999b.  $^{186}\text{Os}$ – $^{187}\text{Os}$  systematics of Hawaiian picrites. *Earth Planet. Sci. Lett.* **174**, 25–42.
- Brandon, A.D., Snow, J.E., Walker, R.J., Morgan, J.W., Mock, T.D., 2000.  $^{190}\text{Pt}$ – $^{186}\text{Os}$  and  $^{187}\text{Re}$ – $^{187}\text{Os}$  systematics of abyssal peridotites. *Earth Planet. Sci. Lett.* **177**, 319–335.
- Brandon, A.D., Walker, R.J., 2005. The debate over core–mantle interaction. *Earth Planet. Sci. Lett.* **232**, 211–225.
- Brandon, A.D., Walker, R.J., Morgan, J.W., Norman, M.D., Prichard, H.M., 1998. Coupled  $^{186}\text{Os}$  and  $^{187}\text{Os}$  evidence for core–mantle interaction. *Science* **280**, 1570–1573.
- Brandon, A.D., Walker, R.J., Puchtel, I.S., Becker, H., Humayun, M., Revillon, S., 2003.  $^{186}\text{Os}$ – $^{187}\text{Os}$  systematics of Gorgona Island komatiites: implications for early growth of the inner core. *Earth Planet. Sci. Lett.* **206**, 411–426.
- Brenker, F.E., Meibom, A., Frei, R., 2003. On the formation of peridotite-derived Os-rich PGE alloys. *Am. Mineral.* **88**, 1731–1740.

- Cabri, L.J., Harris, D.C., 1975. Zoning in Os–Ir alloys and the relation of the geological and tectonic environment of the source rocks to the bulk Pt:Pt + Ir + Os ratio for placers. *Can. Mineral.* **13**, 266–274.
- Cabri, L.J., Harris, D.C., Weiser, T.W., 1996. Mineralogy and distribution of platinum-group mineral (PGM) placer deposits of the world. *Explor. Min. Geol.* **5**, 73–167.
- Chou, C.-L., 1978. Fractionation of siderophile elements in the earth's upper mantle. *Proc. Lunar Planet. Sci. Conf.* **IX**, 219–230.
- Danielson, L.R., Sharp, T.G., Hervig, R.L., 2005. Implications for core formation of the Earth from high pressure-temperature Au partitioning experiments. *Proc. Lunar Planet. Sci. Conf.* **XXXVI**, 1955.
- Hattori, K., Hart, S.R., 1991. Osmium-isotope ratios of platinum group minerals associated with ultramafic intrusions—Os isotopic evolution of the oceanic mantle. *Earth Planet. Sci. Lett.* **107**, 499–514.
- Hauri, E.H., Hart, S.R., 1997. Rhenium abundances and systematics in oceanic basalts. *Chem. Geol.* **139**, 185–205.
- Holzheid, A., Sylvester, P., O'Neill, H.St.C., Rubie, D.C., Palme, H., 2000. Evidence for late chondritic veneer in the Earth's mantle from high pressure partitioning of palladium and platinum. *Nature* **406**, 396–399.
- Horan, M.F., Walker, R.J., Morgan, J.M., Grossman, J.N., Rubin, A.E., 2003. Highly siderophile elements in chondrites. *Chem. Geol.* **193**, 5–20.
- Huss, G.R., Lewis, R.S., 1995. Presolar diamond, SiC, and graphite in primitive chondrites: abundances as a function of meteorite class and petrologic type. *Geochim. Cosmochim. Acta* **59**, 115–160.
- Huss, G.R., 1997. The survival of presolar grains in solar system bodies. In: Bernatowicz, T.J., Zinner, E. (Eds.), *Astrophysical Implications of the Laboratory Study of Presolar Materials*, vol. 402. Proceedings of the American Institute of Physics, New York, pp. 721–748.
- Malitch, K.N., 2004. Osmium isotope constraints on contrasting sources and prolonged melting in the Proterozoic upper mantle: evidence from ophiolitic Ru–Os sulfides and Ru–Os–Ir alloys. *Chem. Geol.* **208**, 157–173.
- McInnes, B.I.A., McBride, J.S., Evans, N.J., Lambert, D.D., Andrew, A.S., 1999. Osmium isotope constraints on ore metal recycling in subduction zones. *Science* **286**, 512–516.
- Meibom, A., Frei, R., 2002. Evidence for an ancient osmium isotopic reservoir in Earth. *Science* **296**, 516–518.
- Meibom, A., Sleep, N.H., Chamberlain, C.P., Coleman, R.G., Frei, R., Hren, M.T., Wooden, J.L., 2002. Re–Os isotopic evidence for long-lived heterogeneity and equilibration processes in the Earth's upper mantle. *Nature* **419**, 705–708.
- Meibom, A., Frei, R., Sleep, N.H., 2004. Osmium isotopic compositions of Os-rich platinum group element alloys from the Klamath and Siskiyou Mountains. *J. Geophys. Res.* **109**, B02203. doi:10.1029/2003JB002602.
- Meisel, T., Walker, R.J., Irving, A.J., Lorand, J.-P., 2001. Osmium isotopic compositions of mantle xenoliths: a global perspective. *Geochim. Cosmochim. Acta* **65**, 1311–1323.
- Meisel, T., Walker, R.J., Morgan, J.W., 1996. The osmium isotopic composition of the Earth's primitive upper mantle. *Nature* **383**, 517–520.
- Morgan, J.W., 1986. Ultramafic xenoliths: clues to Earth's late accretionary history. *J. Geophys. Res.* **91**, 12375–12387.
- Morgan, J.W., Walker, R.J., Brandon, A.D., Horan, M.F., 2001. Siderophile elements in Earth's upper mantle and lunar breccias: data synthesis suggests manifestations of the same late influx. *Met. Planet. Sci.* **36**, 1257–1275.
- Morgan, J.W., Wandless, G.A., Petrie, R.K., Irving, A.J., 1981. Composition of the Earth's upper mantle, I. Siderophile trace elements in ultramafic nodules. *Tectonophysics* **75**, 47–67.
- Murthy, V.R., 1991. Early differentiation of the Earth and the problem of mantle siderophile elements: a new approach. *Science* **253**, 303–306.
- Peck, D.C., Keays, R.R., 1990. Geology, geochemistry, and origin of platinum-group element chromitite occurrences in the Heazlewood River Complex, Tasmania. *Econ. Geol.* **85**, 765–793.
- Peslier, A.H., Reisberg, L., Ludden, J., Francis, D., 2000. Re–Os constraints on harzburgite and lherzolite formation in the lithospheric mantle: a study of Northern Canadian Cordillera xenoliths. *Geochim. Cosmochim. Acta* **64**, 3061–3071.
- Puchtel, I.S., Brandon, A.D., Humayun, M., 2004a. Precise Pt–Re–Os isotope systematics of the mantle from 2.7 Ga komatiites. *Earth Planet. Sci. Lett.* **224**, 157–174.
- Puchtel, I.S., Brandon, A.D., Humayun, M., 2005. Evidence for the early differentiation of the core from Pt–Re–Os isotope systematics of 2.8-Ga komatiites. *Earth Planet. Sci. Lett.* **237**, 118–134.
- Puchtel, I.S., Humayun, M., 2000. Platinum group elements in Kostomuksha komatiites and basalts: implications for oceanic crust recycling and core–mantle interaction. *Geochim. Cosmochim. Acta* **64**, 4227–4242.
- Puchtel, I.S., Humayun, M., Campbell, A., Sproule, R., Leshner, C.M., 2004b. Platinum group element geochemistry of komatiites from the Alexo and Pyke Hill areas, Ontario, Canada. *Geochim. Cosmochim. Acta* **68**, 1361–1383.
- Rehkämper, M., Halliday, A.N., Fitton, J.G., Lee, D.-C., Wieneke, M., Arndt, N.T., 1999. Ir, Ru, Pt and Pd in basalts and komatiites: new constraints for the geochemical behavior of the platinum-group elements in the mantle. *Geochim. Cosmochim. Acta* **63**, 3915–3934.
- Righter, K., 2003. Metal–silicate partitioning of siderophile elements and core formation in the early Earth. *Annu. Rev. Earth Planet. Sci.* **31**, 135–174.
- Righter, K., Drake, M., 1997. Metal–silicate equilibrium in a homogeneously accreting Earth: new results for Re. *Earth Planet. Sci. Lett.* **146**, 553–641.
- Righter, K., Drake, M., Yaxley, G., 1997. Prediction of siderophile element metal–silicate partition coefficients to 20 GPa and 2800 °C: the effect of pressure, temperature, fO<sub>2</sub> and silicate and metallic melt composition. *Phys. Earth Planet. Int.* **100**, 115–134.
- Rushmer, T., Petford, N., Humayun, M., Campbell, A.J., 2005. Fe–liquid segregation in deforming plumes: coupling core-forming compositions with transport phenomena. *Earth Planet. Sci. Lett.* **239**, 185–202.
- Shirey, S.B., Walker, R.J., 1998. The Re–Os isotope system in cosmochemistry and high-temperature geochemistry. *Annu. Rev. Earth Planet. Sci.* **26**, 423–500.
- Smoliar, M.I., Walker, R.J., Morgan, J.W., 1996. Re–Os ages of group IIA, IIIA, IVA, and IVB iron meteorites. *Science* **271**, 1099–1102.
- Stockman, H.W., Hlava, P.F., 1984. Platinum-group minerals in alpine chromitites from southwestern Oregon. *Econ. Geol.* **79**, 491–508.
- Walker, R.J., Brandon, A.D., Bird, J.M., Piccoli, P.M., McDounough, W.F., Ash, R.D., 2005. <sup>187</sup>Os–<sup>186</sup>Os systematics of Os–Ir–Ru alloy grains from southwestern Oregon. *Earth Planet. Sci. Lett.* **230**, 211–226.
- Walker, R.J., Carlson, R.W., Shirey, S.B., Boyd, F.R., 1989. Os, Sr, Nd, and Pb isotope systematics of southern African peridotite xenoliths: implications for the chemical evolution of subcontinental mantle. *Geochim. Cosmochim. Acta* **53**, 1583–1595.
- Walker, R.J., Horan, M.F., Morgan, J.W., Becker, H., Grossman, J.N., Rubin, A.E., 2002. Comparative <sup>187</sup>Re–<sup>187</sup>Os systematics of chondrites: implications regarding early solar system processes. *Geochim. Cosmochim. Acta* **66**, 4187–4201.
- Walker, R.J., Morgan, J.W., Beary, E., Smoliar, M.I., Czamanske, G.K., Horan, M.F., 1997. Applications of the <sup>190</sup>Pt–<sup>186</sup>Os isotope system to geochemistry and cosmochemistry. *Geochim. Cosmochim. Acta* **61**, 4799–4808.
- Walker, R.J., Morgan, J.W., Horan, M.F., 1995. <sup>187</sup>Os enrichment in some mantle plume sources: evidence for core–mantle interaction? *Science* **269**, 819–822.
- Walker, R.J., Shirey, S.B., Stecher, O., 1988. Comparative Re–Os, Sm–Nd, and Rb–Sr isotope and trace element systematics for Archean komatiite flows from Munro Township, Abitibi Belt, Ontario. *Earth Planet. Sci. Lett.* **87**, 1–12.
- Walker, R.J., Storey, M., Kerr, A.C., Tarney, J., Arndt, N.T., 1999. Implications of <sup>187</sup>Os isotopic heterogeneities in a mantle plume: evidence from Gorgona Island and Curacao. *Geochim. Cosmochim. Acta* **63**, 713–728.
- Widom, E., Kepezhinskas, P., Defant, M., 2003. The nature of metasomatism in the sub-arc mantle wedge: evidence from Re–Os isotopes in Kamchatka peridotite xenoliths. *Chem. Geol.* **196**, 283–306.